



HAL
open science

Statistical modelling of digital elevation models for GNSS-based navigation

Hiba Al-Assaad, Christophe Boucher, Ali Daher, Ahmad Shahin, Jean-Charles Noyer

► **To cite this version:**

Hiba Al-Assaad, Christophe Boucher, Ali Daher, Ahmad Shahin, Jean- Charles Noyer. Statistical modelling of digital elevation models for GNSS-based navigation. International Journal of Image and Data Fusion, 2023, pp.1-20. 10.1080/19479832.2023.2218376 . hal-04117736

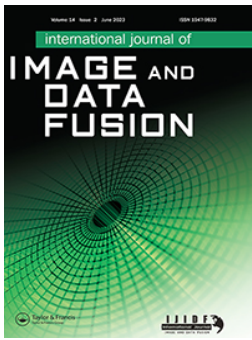
HAL Id: hal-04117736

<https://hal.science/hal-04117736>

Submitted on 5 Jun 2023

HAL is a multi-disciplinary open access archive for the deposit and dissemination of scientific research documents, whether they are published or not. The documents may come from teaching and research institutions in France or abroad, or from public or private research centers.

L'archive ouverte pluridisciplinaire **HAL**, est destinée au dépôt et à la diffusion de documents scientifiques de niveau recherche, publiés ou non, émanant des établissements d'enseignement et de recherche français ou étrangers, des laboratoires publics ou privés.



Statistical modelling of digital elevation models for GNSS-based navigation

Hiba Al-Assaad, Christophe Boucher, Ali Daher, Ahmad Shahin & Jean-Charles Noyer

To cite this article: Hiba Al-Assaad, Christophe Boucher, Ali Daher, Ahmad Shahin & Jean-Charles Noyer (2023): Statistical modelling of digital elevation models for GNSS-based navigation, International Journal of Image and Data Fusion, DOI: [10.1080/19479832.2023.2218376](https://doi.org/10.1080/19479832.2023.2218376)

To link to this article: <https://doi.org/10.1080/19479832.2023.2218376>



Published online: 05 Jun 2023.



Submit your article to this journal [↗](#)



View related articles [↗](#)



View Crossmark data [↗](#)

RESEARCH ARTICLE



Statistical modelling of digital elevation models for GNSS-based navigation

Hiba Al-Assaad ^a, Christophe Boucher ^b, Ali Daher ^c, Ahmad Shahin ^d and Jean-Charles Noyer ^e

^aEngineering school, CESI-LINEACT Laboratory, Labège, France; ^bUniversité du Littoral Côte d'Opale, Laboratoire Informatique Signal Et Image de la Côte d'Opale, Calais Cedex, France; ^cUniversité Libanaise, Faculté de Génie, Centre de Recherche Scientifique En Ingénierie (CRIS), Tripoli, Republic of Lebanon; ^dUniversité Libanaise, Ecole Doctorale En Sciences Et Technologies, Laboratoire d'Informatique Et Ses Applications, Rue Mitein, Tripoli, Republic of Lebanon; ^eEngineering school, Université du Littoral Côte d'Opale, Laboratoire Informatique Signal Et Image de la Côte d'Opale, Calais Cedex, France

ABSTRACT

Recently, smart mobility has become an important activity in transportation systems such as public, autonomous and shared transports. These systems require reliable navigation applications that lead to precise localisation and optimised routes. The GPS system may face problems such as signal degradation caused by conical effects, affecting the reliability and accuracy of the signal, or signal loss in poor visibility environments. By using other sensors, the vehicle location system can overcome these GPS problems. This work focuses on the estimation of the inclination, which will be used to optimise the route planning for the EV or HEV especially in order to control the energy consumption. This paper presents a multi-sensor fusion method, based on GNSS, INS, OSM and DEM data fused using a non-linear particle filter, to estimate and improve the slopes of road segments. A new statistical modelling of the DEM errors related to the spatial sampling of elevation data is proposed. This method is based on the definition of a geometrical window, called Adjacent Sliding Window (ASW), which dynamically selects the elevation data in the vicinity of the road. The proposed method is evaluated in a suburban transport network. The experimental results show the benefits of the vehicle attitude and road slope estimation accuracies.

ARTICLE HISTORY

Received 17 October 2022
Accepted 7 May 2023

KEYWORDS

Intelligent transportation; GNSS-based navigation; digital roadmap and elevation model; particle filtering

1. Introduction

In recent years, smart cities have been working on transitioning to Electric Vehicle (EV) technology due to its environmental benefits and limited energy needs (Quddus *et al.* 2007; Shankar and Marco 2013, Veneri and Veneri 2017, Qu *et al.* 2019). Electric transport can reduce fuel consumption as well as air pollution. However, this technology requires advanced information such as road topology and driving behaviour information (Ohnishi *et al.* 2000, Wang *et al.* 2015, Liao *et al.* 2017, Jiang *et al.* 2019). The inclination of the road is one of the most important

CONTACT Hiba Al-Assaad  halassaad@cesi.fr  Engineering school, CESI-LINEACT Laboratory, 16 Rue Magellan, Labège 31670, France

parameters that is used in these intelligent transport applications. Indeed, it influences the vehicle route planning algorithm that can optimise the energy consumption (Kaul *et al.* 2013, Boucher and Noyer 2014, Patel *et al.* 2016).

There are works that present a solution for determining the positioning accuracy of navigation systems based on the Twice Distance Root Mean Square (2DRMS) (Specht 2021). Also, many works that are interested in the estimation of slopes have been developed in the past. They use geometric, statistical and machine learning approaches. For instance, Ustunel *et al.* presented three methods (geometry-based, local feature-based and covariance-based) for estimating road slopes from instantaneous road images obtained by a front monocular camera (Ustunel and Masazade 2019). However, Korayem *et al.* proposes two approaches for estimating slope and bank angles for vehicles using a model-based and machine learning approach (Habibnejad Korayem *et al.* 2021). A Progressive Recursive Least Squares (PRLS) algorithm for real-time estimation of vehicle mass and road slope is proposed by Ling *et al.* (2021). Slope information can be used in many applications such as Adaptive Cruise Control (ACC) (Wang *et al.* 2021) and speed tracking control for electric vehicles (Zhang *et al.* 2022). It is also used in green transportation methods (bikes, scooters, etc.).

The paper describes a multi-sensor fusion system that is presented as a solution to estimate the navigation parameters of a land vehicle navigate in an open environment. In addition, a novel approach to modelling elevation data is proposed with the aim of improving the accuracy of estimating the vehicle elevation and road segment slopes. This fusion system uses the positioning coordinates delivered by the GNSS (Global Navigation Satellite System), the acceleration and attitude angles readings (Inertial Navigation System (INS) measurements) delivered by the ublox EVK-M8U sensor. **Also, the 2D coordinates and elevation data from digital road map and elevation model are used.** The GNSS/INS measurements are fused with the OpenStreetMap (OSM)¹ database using a matching criterion based on the computation of the Mahalanobis distance (Mahalanobis 1936, Wang *et al.* 2008, Gong *et al.* 2015, Aftatah *et al.* 2016). **This matching step is applied to increase the accuracy of the 2D localisation.** Then, in order to obtain 3D accurate positioning (Al-Assaad *et al.* 2018, Tighe and Chamberlain 2009, Ciepluch *et al.* 2010, Rafone 2013), a Digital Elevation Model (DEM) is used to improve and limit the altitude errors caused by the GNSS system (Boucher and Noyer 2018). **A new statistical modelling method of the errors related to the spatial sampling of elevation data is proposed. The method is based on a model that takes into account the DEM data as a sliding weighted window.** This fusion system benefits from the performance of a Particle Filter (PF) and probabilistic map-matching algorithms to estimate the location and attitude of a vehicle. **Thus, the OSM database that contains a 2D model of the road network, is enriched with the estimated inclination of road sections.** Note that, the work presented in this article is an extended version of the work presented in this paper (Boucher *et al.* 2021).

This method is evaluated in true experimental scenario. Data are obtained from an instrumented vehicle in a context of urban traffic in the city of Calais, France. Results show a high efficiency in estimation road slopes.

2. 3D state modelling

In this estimation method, the three parameters that represent the dynamics of the vehicle are the position, the velocity and the acceleration along the three coordinates x , y and z that are attached to the ENU-UTM (East North Up-Universal Transverse Mercator) navigation frame with z corresponding to the altitude of the EGM96 reference frame. So, let X_k be the following state vector: equation (1)

$$X_k = (x_k, v_k^x, \gamma_k^x, y_k, v_k^y, \gamma_k^y, z_k, v_k^z, \gamma_k^z)^T \quad (1)$$

This method is based on a non-linear filter that deals with sequential correction steps based on GNSS positioning, acceleration and pitch angle measurements. Then, two steps of cartographic correction are applied based on road and elevation maps. This paper presents a general framework for the estimation of 3D vehicle parameters with road slope estimation.

2.1. Dynamics equation

The vehicle dynamics can be described by a third-order kinematic state model along the three coordinates axes $u = \{x, y, z\}$: equation (2)

$$\begin{pmatrix} Y_{k+1}^u \\ v_{k+1}^u \\ u_{k+1}^u \end{pmatrix} = \underbrace{\begin{pmatrix} 1 & 0 & 0 \\ \Delta_k & 1 & 0 \\ 0 & \Delta_k & 1 \end{pmatrix}}_{f_u} \begin{pmatrix} Y_k^u \\ v_k^u \\ u_k^u \end{pmatrix} + \begin{pmatrix} \Omega_k^{y^u} \\ \Omega_k^{v^u} \\ \Omega_k^{u^u} \end{pmatrix} \quad (2)$$

where:

- F_u is the dynamics matrix and Δ_k is a navigation rate of the system,
- $(\Omega_k^{y^u}, \Omega_k^{v^u}, \Omega_k^{u^u})$ are the additive white Gaussian noises. These noises take into consideration the intrinsic correlations between the three components.

Therefore, the matrix form of the 3D dynamics is presented as follows: equation (3)

$$X_{k+1} = f(X_k, \Omega_k) = FX_k + \Omega_k \quad (3)$$

where F is the matrix function of the linear dynamic flow of the system: equation (4)

$$F = \begin{pmatrix} F_x & \emptyset_{3 \times 3} & \emptyset_{3 \times 3} \\ \emptyset_{3 \times 3} & F_y & \emptyset_{3 \times 3} \\ \emptyset_{3 \times 3} & \emptyset_{3 \times 3} & F_z \end{pmatrix} \text{ with } F_x = F_y = F_z = \begin{pmatrix} 1 & 0 & 0 \\ \Delta_k & 1 & 0 \\ 0 & \Delta_k & 1 \end{pmatrix} \quad (4)$$

where $\emptyset_{3 \times 3}$ is a null square matrix of a 3×3 dimension.

2.2. Measurement equations

In this estimation method, the GNSS positions, accelerations, and pitch angle measurements are collected using a u-blox EVK-M8U receiver. Then, the OSM road network and World 30 terrain surface maps are used as supplementary sensors to refine the 2D/3D position.

2.2.1. GNSS measurement

The GNSS measurements are collected using the u-blox EVK-M8U, whose antenna is fixed on the top of the vehicle. The position measurements are expressed in the ENU (UTM) navigation frame. They are noted by $\mathcal{Z}_{k+1}^{\text{GNSS}}$: equation (5)

$$\mathcal{Z}_{k+1}^{\text{GNSS}} = \begin{pmatrix} x_{k+1}^{\text{GNSS}} \\ y_{k+1}^{\text{GNSS}} \\ z_{k+1}^{\text{GNSS}} \end{pmatrix} = H^{\text{GNSS}}(X_{k+1}) + \mathcal{V}_{k+1}^{\text{GNSS}} \quad (5)$$

$H^{\text{GNSS}}(X_{k+1})$ is the linear function of the GNSS measurement and $\mathcal{V}_{k+1}^{\text{GNSS}} \sim \mathcal{N}(0, R_{k+1}^{\text{GNSS}})$ is an additive white Gaussian noise with zero mean and R_{k+1}^{GNSS} the noise covariance matrix.

2.2.2. Acceleration measurement

The accelerations are measured by a triaxial inertial sensor. They are expressed in the body frame of the vehicle. Therefore, they are transformed into the North-East Down (NED) coordinate frame using the well-known rotation matrices. The measurement is denoted $\mathcal{Z}_{k+1}^{\text{ACC}}$ by: equation (6)

$$\mathcal{Z}_{k+1}^{\text{ACC}} = \begin{pmatrix} Y_{k+1}^x \\ Y_{k+1}^y \\ Y_{k+1}^z \end{pmatrix} = H^{\text{ACC}}(X_{k+1}) + \mathcal{V}_{k+1}^{\text{ACC}} \quad (6)$$

where $H^{\text{ACC}}(X_{k+1})$ is the linear function of the acceleration measurement, and $\mathcal{V}_{k+1}^{\text{ACC}} \sim \mathcal{N}(0, R_{k+1}^{\text{ACC}})$ is a white Gaussian noise with zero mean with R_{k+1}^{ACC} the noise covariance matrix.

2.2.3. Pitch angle measurement

In this fusion method, the acquired pitch angle, described in the ENU frame, is used to estimate the road inclination.

The measurement $\mathcal{Z}_{k+1}^{\text{ATT}}$ is written as follows: equation (7)

$$\mathcal{Z}_{k+1}^{\text{ATT}} = (a_{k+1}) = h^{\text{ATT}}(X_{k+1}) + \mathcal{V}_{k+1}^{\text{ATT}} \quad (7)$$

where $h^{\text{ATT}}(X_{k+1})$ is the non-linear measurement function, given by equation (8)

$$h^{\text{ATT}}(X_{k+1}) = \arctan\left(\frac{v_{k+1}^z}{\sqrt{(v_{k+1}^x)^2 + (v_{k+1}^y)^2}}\right) \quad (8)$$

2.2.4. OSM digital road network

In order to increase the accuracy, map matching is done after GNSS and INS measurements correction. Map data are usually extracted from a Geographic Information System (GIS). They are composed of a set of roads modelled by segments (Haklay and Weber 2008). Each road segment is characterised by two end nodes [N1; N2]. Each node is identified by its ground location $(x_{k+1}^{\text{OSM}}, y_{k+1}^{\text{OSM}})$ and its ground orientation $\theta_{k+1}^{\text{OSM}}$, as illustrated in Figure 1.

These map data are established as potential candidates for the measurement equation. Each candidate is modelled as follows: equation (9)

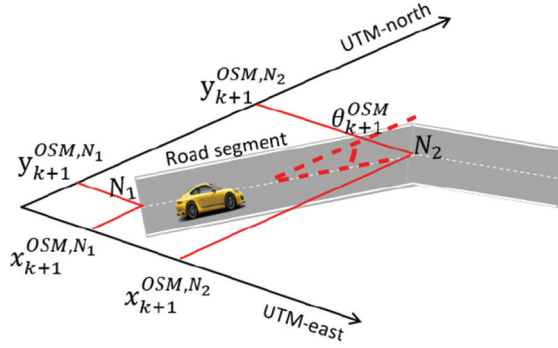


Figure 1. Illustration of OSM road network measurement.

$$\mathcal{Z}_{k+1}^{OSM} = \begin{pmatrix} x_{k+1}^{OSM} \\ y_{k+1}^{OSM} \\ \theta_{k+1}^{OSM} \end{pmatrix} = h^{OSM}(X_{k+1}) + \mathcal{V}_{k+1}^{OSM} \quad (9)$$

$h^{OSM}(X_{k+1})$ is the non-linear measurement function, which relates the state vector to the map measurements, represented by equation (10)

$$h^{OSM}(X_{k+1}) = \begin{pmatrix} x_{k+1} \\ y_{k+1} \\ \arctan\left(\frac{v_{k+1}^y}{v_{k+1}^x}\right) \end{pmatrix} \quad (10)$$

and \mathcal{V}_{k+1}^{OSM} is a white Gaussian noise. This model makes it possible to integrate the statistical aspects of the inhomogeneities cartographic measurement and errors of the terrain. The use of this type of measurements requires the integration of a map-matching step between the GNSS/ACC estimate and the OSM road map.

2.2.5. Elevation terrain surface

The last step of this algorithm is to correct the vehicle altitude. The role of this step is to limit the errors of GNSS altitude measurements. The algorithm fuses the previously estimated parameters, using the OSM road map, with the digital elevation model. Figure 2 illustrates the overall mapping data for the elevation model.

These elevation data are characterised by their location in the ENU ground frame $(x_{k+1}^{DEM}, y_{k+1}^{DEM}, z_{k+1}^{DEM})$. The measurements \mathcal{Z}_{k+1}^{DEM} are modelled as follows: equation (11)

$$\mathcal{Z}_{k+1}^{DEM} = \begin{pmatrix} x_{k+1}^{DEM} \\ y_{k+1}^{DEM} \\ z_{k+1}^{DEM} \end{pmatrix} = h^{DEM}(X_{k+1}) + \mathcal{V}_{k+1}^{DEM} \quad (11)$$

where $h^{DEM}(X_{k+1})$ is the non-linear measurement function that relates the state vector to the measurements of the DEM, presented by: equation (12)

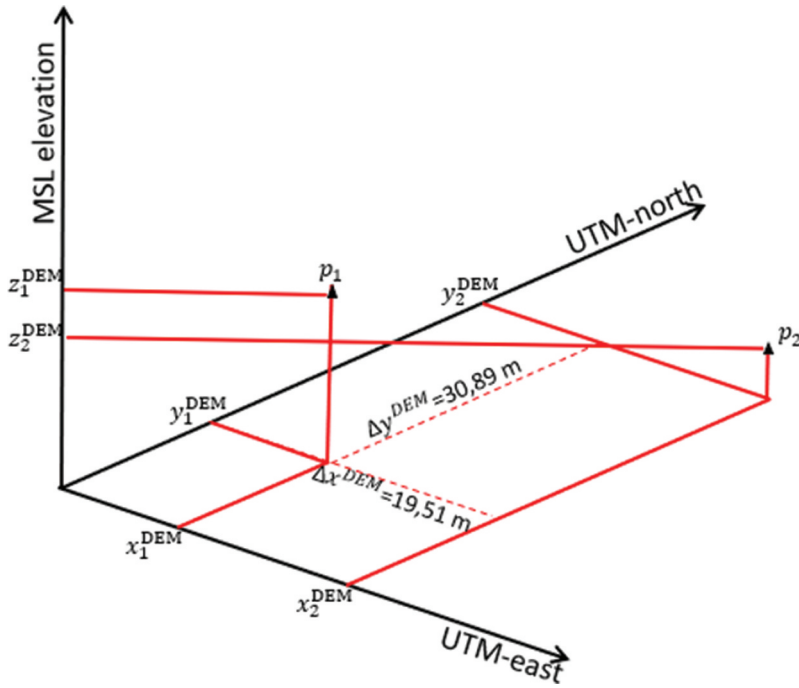


Figure 2. Illustration of the digital elevation model measurements.

$$h^{\text{DEM}}(X_{k+1}) = \begin{pmatrix} x_{k+1} \\ y_{k+1} \\ z_{k+1} - \frac{H}{\cos(\alpha_{k+1})} \end{pmatrix} \quad (12)$$

H denotes the height from the road to the vehicle roof where the EVK-M8U receiver antenna is placed. The term α_{k+1} is the angle between the ground and the road plane at time $k + 1$ [5].

3. Roads inclination estimation

The objective of the proposed method is to estimate the vehicle dynamic parameters with the inclination of the roads in a selected area. After the initialisation of the particles, an evolution step of the state vector is realised. **The GNSS/INS correction steps are based on the GNSS position, acceleration, and pitch angle measurements at time instant.** Then, an OSM correction step is applied to increase the accuracy of 2D localisation based on a map-matching criterion that relies on the computation of Mahalanobis distances. This correction step allows us to select the road segment travelled by the vehicle. The details of GNSS/INS/OSM correction steps are presented in (Al-Assaad *et al.* 2018). Following the 2D OSM-matching step, the DEM correction procedure is applied to determine the elevation zone where the vehicle is driving and the vertical MSL-elevation of the vehicle. This method relies on a TIN (Triangulated Irregular Network) geometric approach (Shunlin *et al.* 2012). **A new method of altitude correction applied for the terrain surface model is introduced in this part. This method is not limited to**

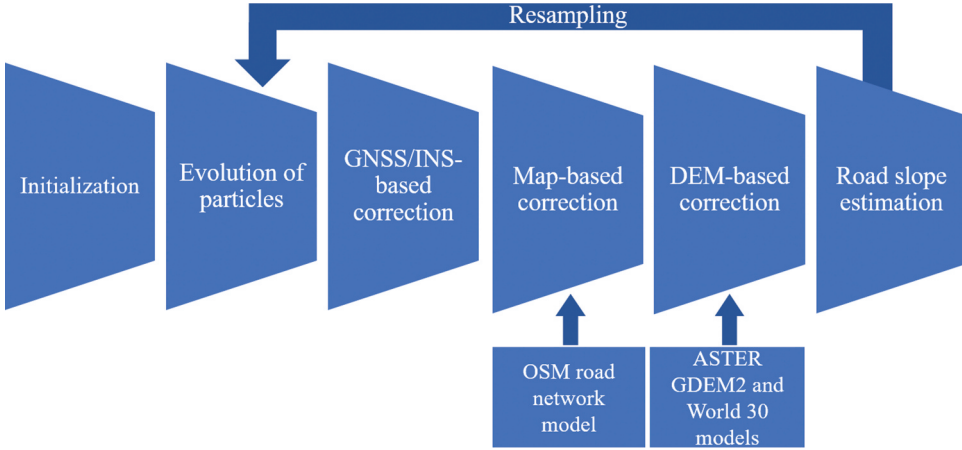


Figure 3. The fusion algorithm structure.

a specific sensor kind or data model. The general structure of the fusion algorithm is shown in Figure 3.

3.1. Initialization and evolution of particles

The particle filter consists in the generation of a set of random measures $\{X_{0:k}^i, w_k^i\}_{i=1}^N$ characterised by the posterior probability density function $p(X_{0:k} | Z_{1:k})$. The set of these particles $\{X_k^i, i = 1, \dots, N\}$ is characterised by a set of associated weights for each particle $\{w_k^i, i = 1, \dots, N\}$. The constant N is the number of particles of a state X_k . The initial weights w_0^i are equal and normalised to $1/N$ for the whole set of particles: equation (13)

$$\sum_{i=1}^N w_k^i = 1 \quad (13)$$

The evolution of a state vector X_{k+1}^i of a vehicle is given by equation (14)

$$X_{k+1}^i = \mathcal{F}X_k^i + \Omega_k^i \quad (14)$$

where :

- \mathcal{F} is the dynamic matrix of the state vector X_k^i at the time k ;
- Ω_k^i is the vector of additive white Gaussian noise.

3.2. General correction principle

The filter uses the GNSS position, acceleration, pitch angle, OSM road network and World 30 terrain surface model to estimate vehicle dynamics. **Each measurement is denote by**, where a represents GNSS, ACC, ATT, OSM and DEM, respectively. The measurement equation can be expressed as equation (15) follows:

$$Z_{k+1}^a = h^a(X_{k+1}) + \mathcal{V}_{k+1}^a \quad (15)$$

The weight calculation step consists to correct the normalised weights of the particles w_{k+1}^i by the available measurement, using the Bayes rule: equation (16)

$$w_{k+1}^i = \frac{P(\mathcal{Z}_{k+1}|X_{k+1}^i)}{\sum_{i=1}^N P(\mathcal{Z}_{k+1}|X_{k+1}^i)} w_k^i \quad (16)$$

The log-likelihood function $V(\mathcal{Z}_{k+1}|X_{k+1}^i)$ is written as follows: equation (17)

$$V(\mathcal{Z}_{k+1}|X_{k+1}^i) \sim \ln(P(\mathcal{Z}_{k+1}|X_{k+1}^i)) \sim \|\mathcal{Z}_{k+1}^\mu - H^\mu X_{k+1}^i\|_{R^\mu}^2 \quad (17)$$

where:

- μ presents the GNSS position data available at the instant $k + 1$;
- $\|\cdot\|_{R^\mu}^2$ is equal to $(\cdot)^T R^{\mu-1} (\cdot)$. Then, the weights of the particles are normalised as follows: equation (18)

$$w_{k+1}^i = \frac{w_{k+1}^i}{\sum_{i=1}^N w_{k+1}^i} \quad (18)$$

3.3. GNSS/ACC/ATT correction

After the initialisation of the particle, three correction steps are applied, starting with the correction based on the GNSS measurement available at time instant using the correction Eq.16. Then, the same equation is used for the two correction steps using the acceleration and attitude measurements.

3.4. OSM-road data integration

After the GNSS/INS integration, the 2D position can be refined by matching it with road network data. This map-matching is based on the correlation of the 2D predicted position with the OSM road database. The intermediate predicted measurement is calculated as follows: equation (19)

$$\hat{\mathcal{Z}}_{k+1/k+1}^{\text{OSM}} = \sum_{i=1}^N w_{k+1}^i h^{\text{OSM}}(X_{k+1}^i) \quad (19)$$

where h^{OSM} is a non-linear function that relates the state vector to the road measurements.

Many methods have been proposed in the literature to refine the ground location $\hat{\mathcal{Z}}_{k+1/k+1}^{\text{OSM}}$ using a road network data. This solution is based on the minimisation of the Mahalanobis distance between the 2D predicted position and each candidate of the OSM road network at time $k + 1$.

Road network data are generally modelled by the interconnected nodes. To refine the map modelling, each candidate for the matching procedure is described by the orthogonal projection of the predicted 2D position onto each road segment in the vicinity of the vehicle, if possible, otherwise by the nearest node to this projection (Figure 4). The set of these orthogonal projections $\mathcal{Z}_m^{\text{OSM}}$ is presented by: equation (20)

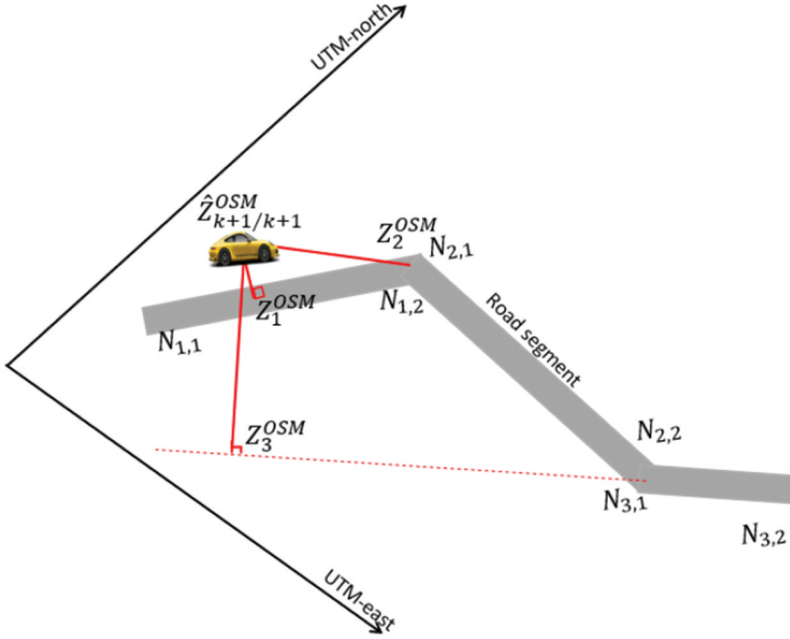


Figure 4. Orthogonal projections on the road network.

$$z_m^{OSM} = \text{proj}_{\perp, m}(\hat{z}_{k+1/k+1}^{OSM}) \quad (20)$$

where $m = \{1, \dots, m_{max}\}$ presents the maximum number of projections onto the road network.

The road measurement also contains the orientation of the road θ_m^{OSM} . The Mahalanobis distance $d_m = d(z_m^{OSM}, \hat{z}_{k+1/k+1}^{OSM})$ is calculated for the two-way direction road (θ_1, θ_2) , presented as follows: equation (21)

$$\begin{cases} z_m^{OSM, \theta_1} = (x_m^{OSM}, y_m^{OSM}, \theta_m^{OSM})^T \\ z_m^{OSM, \theta_2} = (x_m^{OSM}, y_m^{OSM}, \theta_m^{OSM} + \pi)^T \end{cases} \quad (21)$$

Thus, the Mahalanobis distance can be written for (θ_1, θ_2) as follows: equation (22)

$$\begin{cases} (d_{m,k}^{\theta_1})^2 = (D^{\theta_1})^T (\tilde{p}_k^{OSM})^{-1} D^{\theta_1} \\ (d_{m,k}^{\theta_2})^2 = (D^{\theta_2})^T (\tilde{p}_k^{OSM})^{-1} D^{\theta_2} \end{cases} \quad (22)$$

with:

- $D^{\theta_1} = z_{m,k}^{OSM, \theta_1} - \hat{z}_{k+1/k+1}^{OSM}$
- $D^{\theta_2} = z_{m,k}^{OSM, \theta_2} - \hat{z}_{k+1/k+1}^{OSM}$
- Equation (23) \tilde{p}_k^{OSM} presents the error covariance matrix of the predicted road map measurement. It is written as follows:

$$\tilde{p}_k^{\text{OSM}} = \sum_{i=1}^N w_{k+1}^i \left(z_{k+1}^{\text{OSM},i} \right)^2 - \left(\sum_{i=1}^N w_{k+1}^i z_{k+1}^{\text{OSM},i} \right)^2 \quad (23)$$

The OSM correction is applied only if the Mahalanobis distance is less than the constraint of a threshold value ε : equation (24)

$$d_m^\theta \left(z_m^{\text{OSM}}, \hat{z}_{k+1/k+1}^{\text{OSM}} \right) \varepsilon \quad (24)$$

The z_m^{OSM} measure that minimises this criterion is used to correct the prediction estimation after GNSS/INS integration. **After the measurement has been determined, the particle weights w_{k+1}^i are recalculated using the log-likelihood Eq.16, where μ represents the OSM measure z_{k+1}^{OSM} .** Then, the normalise step is applied using Eq. 18.

3.5. Adjacent sliding window method

One of the original contributions of this work is the use of DEMs in the estimation of road parameters, and in particular of their 3D orientation (inclination). This method, based on a particle filtering approach, exploits the DEM elevations to fuse them with the 2D/3D measurements delivered by the GPS/INS/MAP sensors integrated on the vehicle.

Since GNSS elevation measurements are known to be inaccurate, the method proposes to integrate the DEM as a new database providing spatially distributed measurements to limit this error. The proposed non-linear filter enables to consider a dynamic management of the DEM measurements by associating only the spatial discretisation points adapted to the road travelled by the vehicle. By doing so, this approach allows to take into account the topology in the immediate neighbourhood of the road by integrating weighting masks whose geometry can be easily adapted in a dynamic way.

A new statistical approach, called the Adjacent Sliding Window (ASW) method, is proposed to improve the estimation of vehicle elevation and road inclination. The principle of the ASW method is based on a correlation of the road data (road on which the vehicle is travelling) with the topology of the associated terrain (digital elevation model). This method allows a selective approach of the DEM by focusing on the neighbourhood of the area travelled by the vehicle. It includes two steps: first, the selection of the elevation points surrounding the road segment and then, the computation of the new altitude measurement using these elevations.

The shape and size of the window as well as the number of selected points vary depending on the point selection method. **This method is adaptable to any kind of elevation model.** Fig. 5, 6, 7 and 8 show the elevation data, with a road segment presented by its two ends [N1; N2] and the selected DEM points, presented in red colour. The M-point is the intermediate predicted position.

These figures represent, respectively, the selection by an empty rectangle, a full rectangle, a rectangular sliding windows and an ASW around the road segment. In the experimentation, the first three methods do not select the optimum elevation points. The selection points are far from the segment in the first method, but in the two other methods, they are points that do not represent the ground reality because they are away from the road segment. **Therefore, the ASW method was used to**

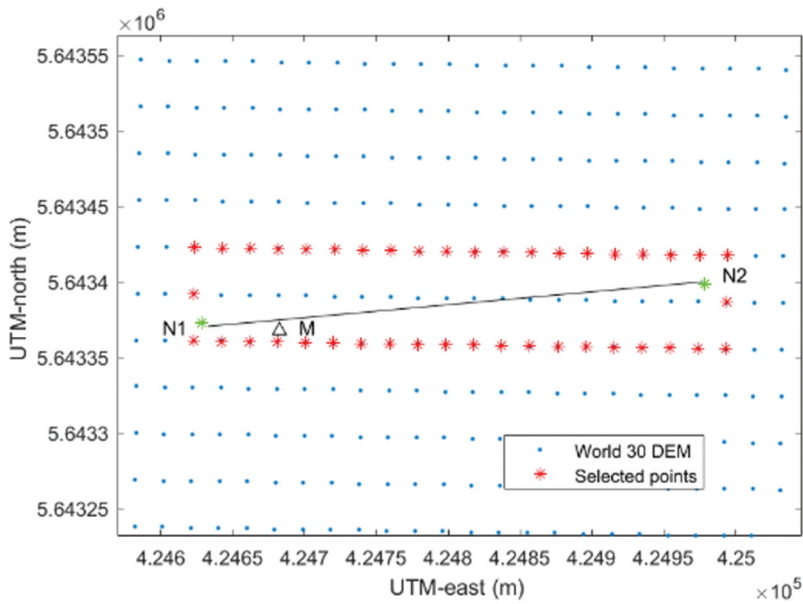


Figure 5. Example of points selection method: empty rectangle.

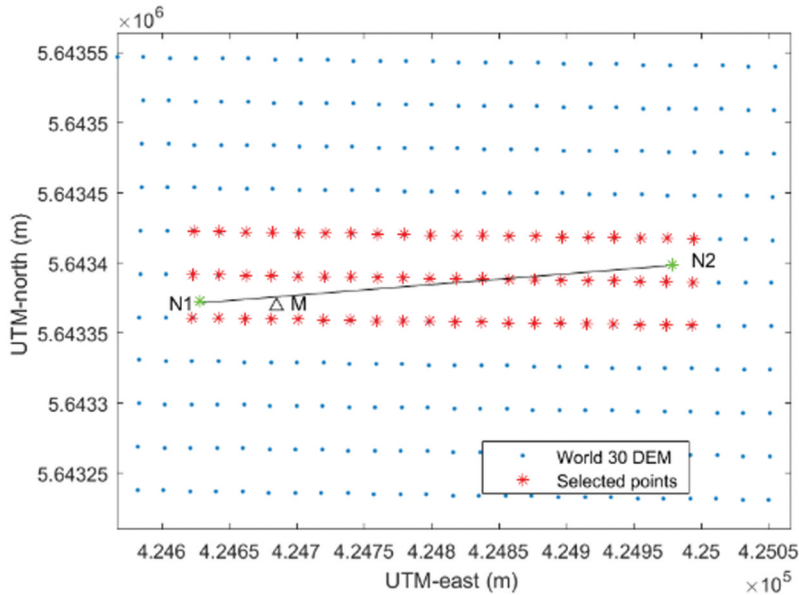


Figure 6. Example of points selection method: full rectangle.

achieve a more precise estimation of altitude. This method selects the points closest to the road segment using the sliding window that traverses the segment. In [Figure 7](#), the points, circled in black, represent the points that are not taken into the ASW method.

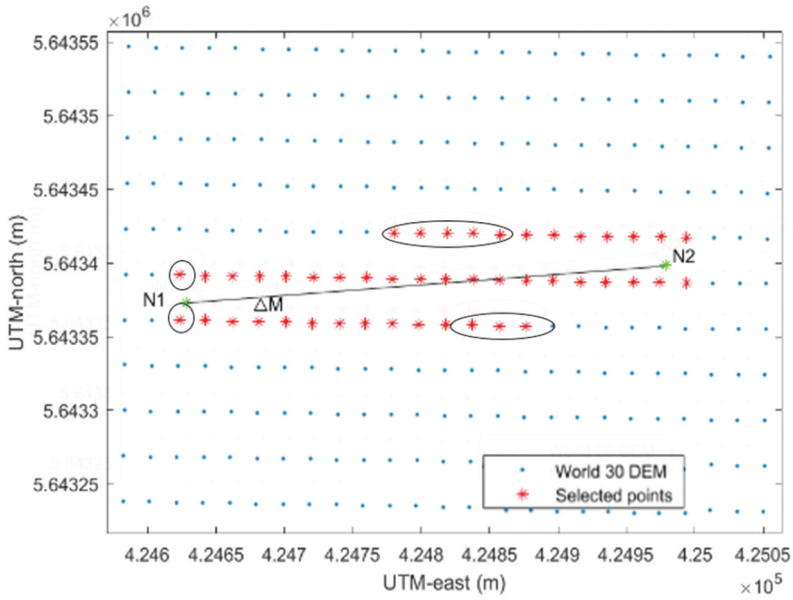


Figure 7. Example of points selection method: rectangular sliding window.

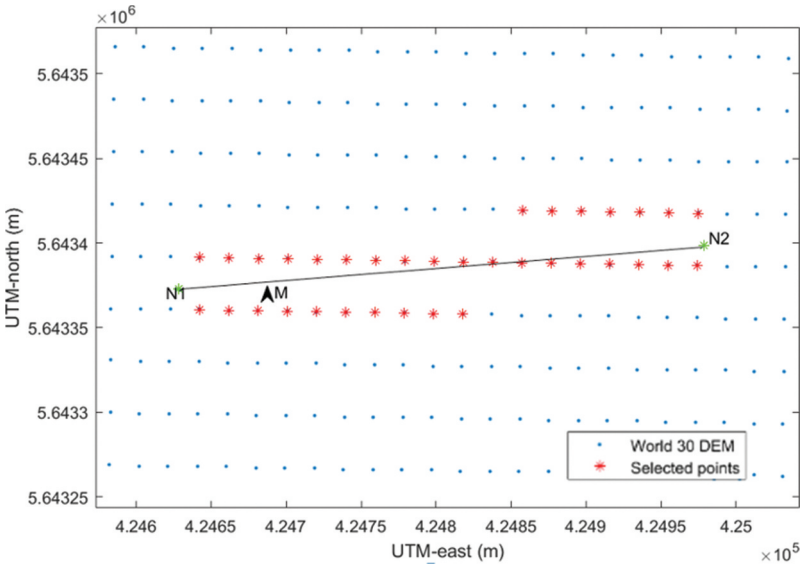


Figure 8. Example of points selection method: adjacent sliding window.

The selected points $(x_i, y_i, z_i)_{i=1, \dots, m}$ can be represented in a 3D plane by equation (25)

$$Z_m^{\text{DEM}} = \{X_{k+1}^{\text{DEM}, i}\}_{i=1}^m \quad (25)$$

A least squares method is employed to establish a correlation between the predicted measurement and the elevation measurements, which enables the computation of the

parameters of the 3D mean plan equation defining this set of points. The following equation is used to calculate the z elevation of the predicted measurement using the 2D position equation (26):

$$z = a.\hat{x}_{k+1/k+1}^{\text{DEM}} + b.\hat{y}_{k+1/k+1}^{\text{DEM}} + c \quad (26)$$

This elevation measure is used to correct the weight of the particle through equation (16), where μ represents the elevation measurement z . Then, the normalisation step is applied using equation (18).

3.6. State vector estimation

After the GNSS/INS/OSM/World 30 data integration, the state vector \hat{X}_{k+1} of the vehicle at time instant $k + 1$ is estimated as follows: equation (27)

$$\hat{X}_{k+1} = \sum_{i=1}^N w_{k+1}^i X_k^i \quad (27)$$

4. Experiments results

The proposed method is tested in a real framework using OSM et DEM data. Maps enhancements are presented here by focusing on road features estimation. The objective of using this map is to take advantage of its accuracy to improve the estimation of roads inclination (Jacobsen 2014, Klomp *et al.* 2014, Arungwa *et al.* 2018). The experimentation context is shown in Figure 9.



Figure 9. Experimental context.

4.1. Experiments configuration

The test vehicle is equipped with a u-blox EVK-M8U sensor for collecting the GNSS/INS data, at 1Hz navigation rate. The receiver is placed on the top of the vehicle with $H = 1.55$ m. The OSM dataset consists of 417 road segments modelled by 73 polylines. A JOSM editor is used to extract the cartography data. The vehicle is driven on this portion of this map and in the same experimental context as in Al-Assaad et al. (2018). In this article, two terrain surface models ASTER GDEM2² et World 30³ are used. These two datasets contain a grid of 14,560 MSL-points with a 30 m ground sampling distance. ASTER GDEM2 data are accompanied with a quality parameter that refers to the measurement accuracy of the elevation. The World 30 model is a fused data model using corrected public data as input, such as Shuttle Radar Topographic Mission (SRTM), ASTER GDEM, and GTOPO30 data. For this reason, this model provides seamless and more accurate information about the elevation data. The data acquisition lasted for a total of 549 s.

To verify the efficiency and robustness of this estimation method, we performed the acquisition on both straight roads and curves. The experiment is conducted in a suburban area. The trajectory starts with an ascending slope to take the A216 highway, then a steep downward slope (about 90 degrees) to join the A16 highway and finally make an ascending turn to return to the starting point by taking the same path but in the opposite direction. The average speed reached by the vehicle is 60 km/h.

4.2. Results of 3D localisation

Figure 10 shows the comparison of the elevation profiles of the GNSS measurements, the value of elevation estimated by the ASW method and the road elevation. Here, the differences in elevation are explained by the location of the receiver antenna on the roof of the vehicle and the height of the road. These results show the effectiveness of the ASW method in detecting elevation variation when changing road segments and the presence of ascending/descending slopes. For example, this method has detected the variation of slopes between $t = 250$ s and $t = 300$ s.

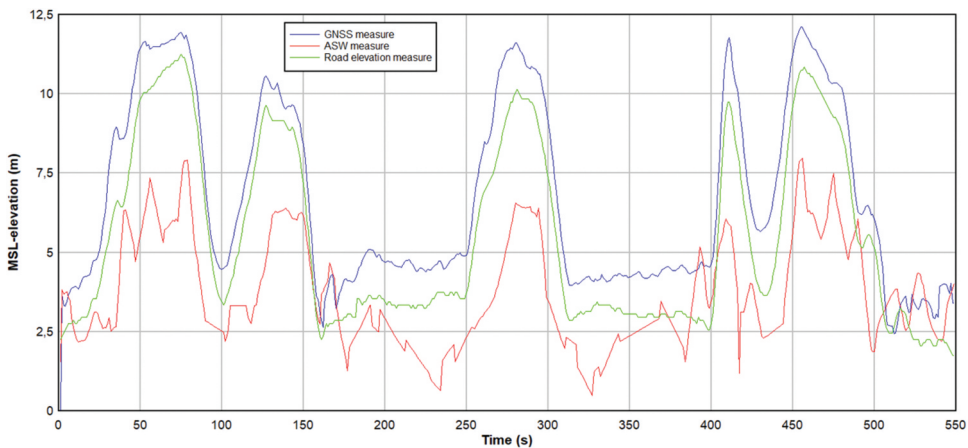


Figure 10. Elevation profiles of GNSS/ASW/road elevation measurements.

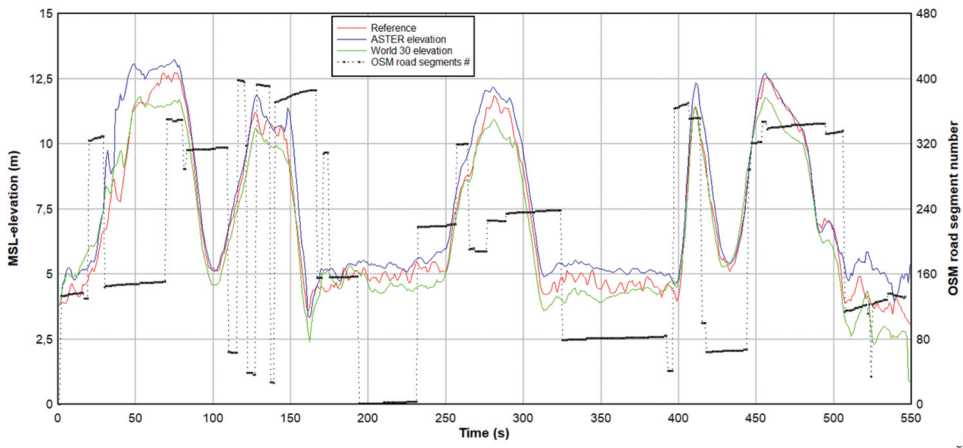


Figure 11. Comparison of ASTER/World 30 altitude estimates.

The comparison of the altitude estimation results obtained by the particle filter using successive GNSS/ACC/OSM/ASTER corrections and those of the particle filter using GNSS/INS/OSM/World 30 corrections is shown in Figure 11. Moreover, all matched OSM road segments numbers are plotted. The vehicle travelled through interchanges that have both ascending and descending slopes.

The ASW method using the World 30 DEM shows elevation variations closer to the reference than the ASTER GDEM2. The computed error statistics give standard deviations of 30 cm for the MSL elevation estimated using the World 30 data instead of 60 cm with the ASTER data. This gain in elevation estimation also affects the overall 3D position estimation. An improvement in the estimation of elevation measurements has been noticed following the refinement of the selection of elevation points. This improvement directly affects the estimation of the slopes.

4.3. Road segment inclination

The least squares method is used to estimate the slope of the roads. It requires to identify the segment travelled by the vehicle in the OSM database and the estimated elevation of the vehicle. As detailed in (Boucher and Noyer 2018), at least four consecutive GNSS instants on the segment are needed to improve the road slope estimation. Fig. 12 shows the estimation results of the all roads inclination percentage for the two elevation maps: ASTER GDEM2 and World 30. **The results show a coherence between the estimates of the slopes between the two models.**

However, it is hard to compare ASTER-based and World30-based estimation accuracies since no ground truth is available concerning the road slopes. However, a heuristical comparison can be derived from the experimental results. Indeed, the A16 highway consists in the segments #83 to #79 (as shown in Figure 13). At this location, the A16 highway is flat, following the recording profile. Therefore, the estimates using the World 30 model are more accurate than the estimates using the ASTER model. However, in the opposite direction of circulation, the two models present similar results (for the segments #156, #157, #1 and #2).

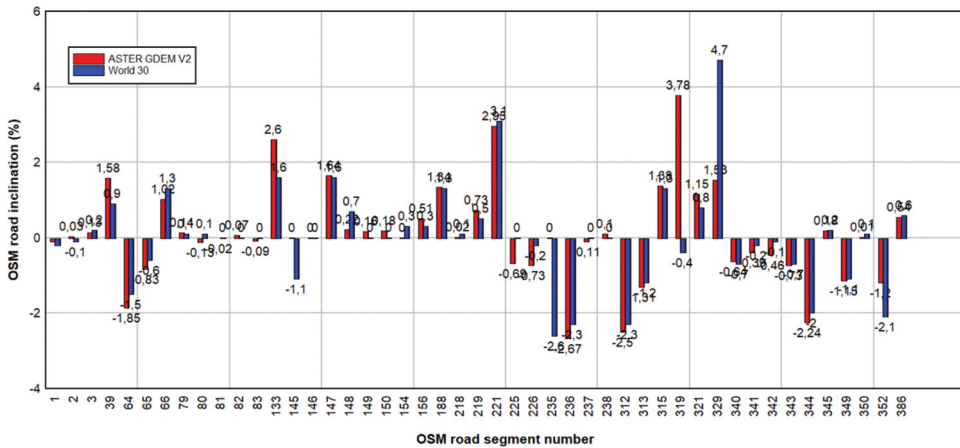


Figure 12. OSM roads inclination.

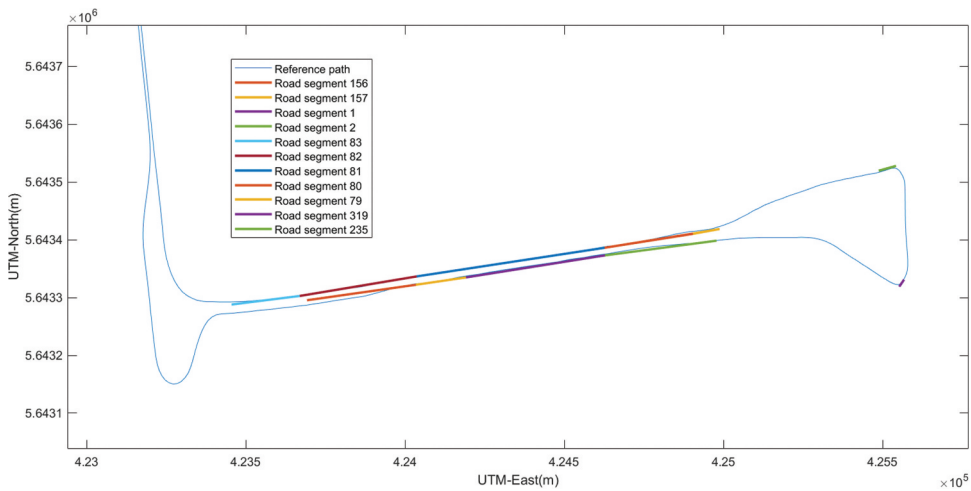


Figure 13. The reference path of the vehicle with OSM road network.

Moreover, the results show a significant difference between the slope estimates for segment #319. As can be seen in Figure 14, the segment #319 is located on the bridge where the road slope is close to zero. The World 30-based estimation is far more accurate (approximately equal to -0.4%) whereas the Aster-based estimate is approximately equal to 3.78% (as shown in Figure 12). The same remark can be done for the segment #235 (as shown in Figure 14), the World 30-based estimation accuracies are closer to the experimental values than the ASTER-based ones.

It shows the efficiency of **the** method for estimating road slopes regardless of the topological variations. The number of altitudes, the length of the road segment, the vehicle speed, and the GNSS/INS measurement frequency are the parameters that affect the accuracy of the slope estimation.



Figure 14. Representation of two road segments 319 and 325.

5. Conclusion

This paper presents a method to estimate roads inclination to enrich the OSM database. This parameter has an impact on the management of the energy consumption for the hybrid/electric vehicle (HEV/EV) (Anselma *et al.* 2019, Guessouri 2019; Jo 2013) and on the route planning applications. The proposed algorithm is based on the fusion of GNSS positioning, INS, OSM road network and DEM. This approach relies on particle filtering that fuses data sequentially in order to estimate the heading and pitch angles of the vehicle. It uses a probabilistic map-matching method based on the calculation of Mahalanobis distance to identify the travelled road of the OSM road network. **This paper presents a general framework to improve the estimation of vehicle altitude and road segment slopes. It uses a statistical modelling based on a weighted window principle to select the optimal elevation measurements taking into account the variation of the topology around the road segment. This modelling is suitable for other elevation models that are considered as new sensors providing new elevation measurements.** The ability of this method to estimate the road slopes travelled by the vehicle has been shown on real data in a suburban environment. Then, these slope estimates will be used to enrich the OSM database. It can be noted that the road slope estimates can also be used to enrich the OSM database and then to procure better experience and information for route planning softwares.

Notes

1. OSM : OpenStreetMap, <https://www.openstreetmap.org>
2. ASTER GDEM2 : Advanced Spaceborne Thermal Emission and Reflection Radiometer Global Digital Elevation Map version 2, <https://asterweb.jpl.nasa.gov/gdem.asp>
3. World 30 : NEXTMap World 30™ Digital Surface Model, <https://www.intermap.com/nextmap>

Acknowledgments

The authors would like to thank Roge Holman of Intermap Technologies for providing samples of the NEXTMap® World 30™ Digital Surface Model (DSM) used in this research work.

Disclosure statement

No potential conflict of interest was reported by the author(s).

Funding

This research was cofunded by Université du Littoral Côte d'Opale (France) and Université Libanaise (Lebanon).

ORCID

Hiba Al-Assaad  <http://orcid.org/0000-0003-1545-7022>
 Christophe Boucher  <http://orcid.org/0000-0002-6070-411X>
 Ali Daher  <http://orcid.org/0000-0002-8277-2068>
 Ahmad Shahin  <http://orcid.org/0000-0003-4704-3035>
 Jean-Charles Noyer  <http://orcid.org/0000-0003-1732-3108>

References

- Aftatah, M., *et al.*, 2016. GPS/INS/Odometer data fusion for land vehicle localization in gps denied environment. *Modern Applied Science*, 11 (1), 62–65. doi:10.5539/mas.v11n1p62.
- Al-Assaad, H., Boucher, C., Daher, A., Shahin, A., Noyer, J.-C., *et al.*, 2018. Fusion of GPS/OSM/DEM data by particle filtering for vehicle attitude estimation. In: H. Al-Assaad, ed. *21st International Conference on Information Fusion (FUSION) 2018*. Cambridge, 384–390.
- Anselma, P.G., 2019. Slope-weighted energy-based rapid control analysis for hybrid electric vehicles. *IEEE Transactions on Vehicular Technology*. Finland, 4458–4466.
- A, Q.M., Ochieng, W.Y., and Noland, R.B., 2007. Current map-matching algorithms for transport applications: state-of-the art and future research directions, *Transp. Res Part C*, 15 (5), 312–328. doi:10.1016/j.trc.2007.05.002.
- Arungwa, I.D., Obarafo, E.O., and Okolie, C., 2018. Validation of global digital elevation models in Lagos state, Nigeria. *Nigerian Journal of Environmental Sciences and Technology (NIJEST)*, 2 (1), 78–88. doi:10.36263/nijest.2018.01.0058.
- Boucher, C., *et al.*, 2021. DEM Embedding in GNSS-Based Navigation Using a Statistical Modeling. *engineering proceedings*, 6, 74. doi:10.3390/I3S2021Dresden-10100
- Boucher, C. and Noyer, J.C., 2014. Automatic estimation of road inclinations by fusing GPS readings with OSM and ASTER GDEM2 data. *IEEE International Conference on Connected Vehicles and Expo ICCVE*. Vienna, Austria, 871–876.
- Boucher, C. and Noyer, J.C., 2018. A general framework for 3-D parameters estimation of roads using GPS OSM and DEM data. *Sensors*, 18 (2), 41. doi:10.3390/s18010041.
- Ciepluch, B., 2010. Comparison of the accuracy of OpenStreetMap for Ireland with google maps and Bing maps. *Proceedings of the Ninth International Symposium on Spatial Accuracy Assessment in Natural Resources and Environmental Sciences 20-23rd*. Leicester, England, 337–340.
- Gong, Y., Zhu, Y., and Yu, J.D.: Detecting elevation of urban roads with smartphones on wheels; Proceedings of the 2015 12th Annual IEEE International Conference on Sensing, Communication, and Networking (SECON); Seattle, WA, USA. 22–25 June 2015, pp. 363–371.

- Guessouri, N. Etude comparative entre influence des différents paramètres physiques et la performance du véhicule électrique modélisation et simulation. 2019.
- Habibnejad Korayem, A., Khajepour, A., and Fidan, B., 2021. Road angle estimation for a vehicle-trailer with machine learning and system model-based approaches. *Vehicle System Dynamics*, 60 (10), 1–22. doi:10.1080/00423114.2021.1969416.
- Haklay, M. and Weber, P., 2008. OpenStreetMap: user-generated street maps. *IEEE Computer SOC Pervas Comput*, 7 (4), 12–18. doi:10.1109/MPRV.2008.80.
- Jacobsen, K., 2014. Performance of large area covering height models. *European Remote Sensing, XL-1/W1*, 1–8. doi:10.5194/isprsarchives-XL-1-W1-157-2013
- Jiang, S., et al., 2019. Adaptive estimation of road slope and vehicle mass of fuel cell vehicle. *ETransportation*, 2, 100023. doi:10.1016/j.etrans.2019.100023
- Jo, K., Kim, J., and Sunwoo, M., 2013. Real-time road-slope estimation based on integration of onboard sensors with gps using an IMM-PDA filter. *IEEE Transactions on Intelligent Transportation Systems*, 14 (4), 1718–1732. doi:10.1109/TITS.2013.2266438.
- Kaul, M., Yang, B., and Jensen, C.S., 2013. Building accurate 3D spatial networks to enable next generation intelligent transportation systems. In: M. Kaled. *IEEE 14th International Conference on Mobile Data Management (MDM)*. Milan, Italy, Vol. 1, 137–146.
- Klomp, M., Gao, Y., and Bruzelius, F., 2014. Longitudinal velocity and road slope estimation in hybrid electric vehicles employing early detection of excessive wheel slip. *Vehicle System Dynamics*, 52 (1), 172–188. doi:10.1080/00423114.2014.887737.
- Liao, X., Huang, Q., Su, D., Weining, L., Weijian, H., et al., 2017. Real-time road slope estimation based on adaptive extended Kalman filter algorithm with in-vehicle data. In: X. Liao ed. *IEEE 29th Chinese Control and Decision Conference (CCDC)*. Bizkaia, Spain, 6889–6894.
- Ling, H., Huang, B., and Jin, X., 2021. Research on torque distribution of four-wheel independent drive off-road vehicle based on PRLS road slope estimation. *Mathematical Problems in Engineering*, 2021, 1–11. doi:10.1155/2021/5399588
- Mahalanobis, P.C., 1936. On the generalized distance in statistics. *Springer Proceedings of the National Institute of Science of India*, 2 (1), 49–55.
- Ohnishi, H., et al., 2000. A study on road slope estimation for automatic transmission control. *Elsevier JSAE Review*, 21 (2), 235–240. doi:10.1016/S0389-4304(99)00097-1.
- Patel, A., Katiyar, S., and Prasad, V., 2016. Performances evaluation of different open source DEM using Differential Global Positioning System (DGPS). *Elsevier the Egyptian Journal of Remote Sensing and Space Science*, 19 (1), 7–16. doi:10.1016/j.ejrs.2015.12.004.
- Qu, L., Zhuang, W., and Chen, N., 2019. Instantaneous velocity optimization strategy of electric vehicle considering varying road slopes. In: W. Zhuang ed. *IEEE Chinese Control and Decision Conference (CCDC)*. Yichang, China, 5483–5488.
- Rafone, E., 2013. Road slope and vehicle mass estimation for light commercial vehicle using linear Kalman filter and RLS with forgetting factor integrated approach. In: E. Rafone ed. *IEEE Proceedings of the 16th International Conference on Information Fusion*. Istanbul, Turkey, 1167–1172.
- Shankar, R. and Marco, J., 2013. *Method for estimating the energy consumption of electric vehicles and plug-in hybrid electric vehicles under real-world driving conditions*. Cardiff, United Kingdom: IET Intelligent Transport Systems, 138–150.
- Shunlin, L., Xiaowen, L., and Jindi, W., 2012. Chapter 2 - Geometric Processing and Positioning Techniques. In: L. Shunlin ed. *Advanced Remote Sensing*. Boston: Academic Press, 33–74.
- Specht, M., 2021. Determination of navigation system positioning accuracy using the reliability method based on real measurements. *Remote Sensing*, 13 (21), 4424. doi:10.3390/rs13214424.
- Tighe, M.L. and Chamberlain, D. Accuracy comparison of the SRTM, ASTER, NED, NEXTMAP USA digital terrain model over several USA study sites. Technical Report Intermap Technologies : Englewood, CO, USA, 2009.
- Ustunel, E. and Masazade, E., 2019. Vision-based road slope estimation methods using road lines or local features from instant images. *IET Intelligent Transport Systems*, 13 (10), 1590–1602. doi:10.1049/iet-its.2018.5479.

- Veneri, O. and Veneri, O., 2017. *Technologies and applications for smart charging of electric and plug-in hybrid vehicles*. Springer. doi:[10.1007/978-3-319-43651-7](https://doi.org/10.1007/978-3-319-43651-7).
- Wang, F.X., 2021. Adaptive cruise control for intelligent city bus based on vehicle mass and road slope estimation. *Applied Sciences*, 11 (24), 12137. doi:[10.3390/app112412137](https://doi.org/10.3390/app112412137).
- Wang, J., Besselink, I., and Nijmeijer, H., 2015. Electric vehicle energy consumption modelling and prediction based on road information. *World Electric Vehicle Journal*, 7 (3), 447–458. doi:[10.3390/wevj7030447](https://doi.org/10.3390/wevj7030447).
- Wang, C., Hu, Z., and Uchimura, K. A precise road network modeling and map matching for vehicle navigation, in Proc. 11th Int. IEEE Conf. Intell. Transp. Syst, Beijing, China, Oct. 2008, pp. 1084–1089.
- Zhang, J., 2022. Robust speed tracking control for future electric vehicles under network-induced delay and road slope variation. *Sensors*, 22 (5), 1787. doi:[10.3390/s22051787](https://doi.org/10.3390/s22051787).